Geoderma 326 (2018) 42–55

Contents lists available at ScienceDirect

Geoderma

journal homepage: www.elsevier.com/locate/geoderma

Spatial and temporal variations of airborne dust fallout in Khorasan Razavi Province, Northeastern Iran

Atefeh Ziyaee[a], Alireza Karimi[a,*], Daniel R. Hirmas[b], Martin Kehl[c], Amir Lakzian[a], Hossein Khademi[d], David B. Mechem[b]

[a] Department of Soil Science, Faculty of Agriculture, Ferdowsi University of Mashhad, 91779-48974, Mashhad, Iran
[b] Department of Geography and Atmospheric Science, University of Kansas, P.O. Box 66045-7613, Lawrence, KS, USA
[c] Institute of Geography, University of Cologne, Albertus-Magnus-Platz, 50923, Cologne, Germany
[d] Department of Soil Science, College of Agriculture, Isfahan University of Technology, Isfahan 84156-83111, Iran

ARTICLE INFO

Handling Editor: M. Vepraskas

Keywords:
Fallout rate
Climatological factors
Playa
Source
Dust storm

ABSTRACT

Dust deposition rates depend mainly on the rate of dust supply, climatic conditions, and topography in the source and sink areas. The objective of this study was to investigate the role of these variables in the spatial and temporal variation of airborne dust fallout in Khorasan Razavi Province, Northeast Iran. Airborne dust samples were collected monthly from May 2014 to April 2015. Dust fallout rate was modelled as a function of air temperature, precipitation, relative humidity, wind velocity and distance from source regions. The lowest and highest rates of atmospheric dust fallout occurred in December and June, with average amounts of 9.97 $g\,m^{-2}$ and 20.96 $g\,m^{-2}$, respectively. The strongest winds were observed in June immediately following a relatively humid period (i.e., March–May) with considerably higher precipitation and lower evaporation. Spatial distributions showed that the highest dust fallout rates occurred in the southern and western parts of the province—areas adjoining the vast playas. During the spring and summer season, the distance from the nearest playa was a key factor that explained more of the variation in dust flux than climatic parameters. Both runoff by fresh sediment moved onto the surface of the playa and the formation of loose sediment on the surfaces of wet playas are mechanisms that can increase dust emissions. The lowest deposition rates were observed in the mountainous region in the north of the province likely due to higher precipitation, atmospheric humidity, and soil moisture. This work represents the first baseline dust data for Khorasan Razavi Province and may be useful in evaluating the effects of future land use and climate change on aeolian land surface processes.

1. Introduction

Airborne dust poses serious human health hazards and environmental risks in arid and semiarid regions (Griffin et al., 2001; Wiggs et al., 2003; Yu et al., 2012), where a lack of continuous vegetative cover makes surface sediments susceptible to wind erosion (Shao, 2008). In these areas, dust is generated by strong prevailing winds ($> 8\,m\,s^{-1}$) that erode sediment from the land surface (Engelstaedter et al., 2006; Xuan et al., 2004). This sediment is carried by these winds and ultimately accumulates on other parts of the landscape via dry or wet deposition or is carried off to other regions where it can have considerable influence over ecosystems (Groll et al., 2013; McTainsh, 1999). Most of this dust (> 80%) is emitted from natural surfaces (Chow et al., 1994), although anthropogenic dust emissions are considerable, especially in populous urban settings (Grobéty et al., 2010).

Various factors contribute to dust deflation and deposition and, thus, control the regional distribution of dust; these factors include surface roughness, vegetation cover, soil properties (e.g., moisture, texture, induration, structure and mineralogy) and topographic features (Engelstaedter et al., 2006; Hirmas et al., 2011; Reheis and Kihl, 1995; Reynolds et al., 2009; Xuan et al., 2004). Playas are susceptible to wind erosion making them arguably the most important sources for dust in arid regions (Cahill et al., 1996; Gill, 1996; Gill et al., 2002; Goudie and Middleton, 2006). Proximity to these landscape features likely controls the distribution of dust (e.g., Hirmas and Graham, 2011). For instance, Liu et al. (2011) studied the rate of airborne dust fallout in the Xinjiang region of China and found that dust fallout decreased with increasing distance from the source playa. This was attributed to increasing distance from the presence of recently deposited sediments and the formation of loose salt minerals on the playa surface which are susceptible

* Corresponding author.
E-mail addresses: at_zi696@mail.um.ac.ir (A. Ziyaee), karimi-a@um.ac.ir (A. Karimi), hirmas@ku.edu (D.R. Hirmas), kehlm@uni-koeln.de (M. Kehl), lakzian@um.ac.ir (A. Lakzian), hkhademi@cc.iut.ac.ir (H. Khademi), dmechem@ku.edu (D.B. Mechem).

https://doi.org/10.1016/j.geoderma.2018.04.010
Received 19 November 2017; Received in revised form 26 March 2018; Accepted 8 April 2018
Available online 19 April 2018
0016-7061/

to wind erosion following desiccation.

In recent years, many studies have been carried out on the temporal variability of dust to better understand aeolian and land surface processes (Engelbrecht and Jayanty, 2013; Flagg et al., 2014; Wang et al., 2009). For example, Groll et al. (2013) reported that peak dust rates in Central Asia between 2003 and 2010 occurred in February and June. They noted that the high dust deposition during the late winter months was likely due to the Siberian high-pressure system which affects regional weather patterns. Additionally, the highest deposition rate during late spring and early summer was related to seasonal warming of the Tibetan Plateau. Marx and McGowan (2005) reported that the highest rates of dust deposition along a 300-km section of the humid west coast of South Island, New Zealand, occurred in the summer due to the reduction in precipitation and abundance of winds capable of carrying airborne dust.

During the past decade, increasing awareness of the human health hazards posed by dust in Iran has spurred investigations documenting the deposition and source areas of the dust and identifying the regional atmospheric and land surface processes controlling dust transport. Hojati et al. (2012) investigated the characteristics of airborne dust along a topographic transect from Jandagh in the Kavir Desert to Kouhrang in the Zagros Mountains of western Iran and concluded that the rate of dust deposition was influenced by both elevation and climate. They also examined distance from the Kavir Desert as a factor affecting dust deposition and found it to be significant. Rashki et al. (2012) analyzed the characteristics of atmospheric airborne dust in the Sistan region in two locations near the Hamoon Lake in eastern Iran during the period between August 2009 and July 2012. The authors reported that the transfer of airborne dust depended mainly on the time of wind occurrence, wind speed and distance from the source. Similarly, Mahmoudi (2011), and Norouzi and Khademi (2015) in Isfahan Province and Jaafari and Khademi (2015) in Kerman Province found significant relationships between dust deposition rates and some climatic parameters such as wind speed, minimum and maximum temperature and average humidity.

Despite the previous research in Iran, the role of landscape-scale and regional atmospheric processes on the distribution and concentration of modern dust is only poorly understood in Khorasan Razavi Province in northeastern Iran which covers approximately 7.8% of the country (Fig. 1). This is unfortunate since this province is unique in that it contains a combination of arid and hyper-arid climates, vast playas, and arid mountain ranges, is affected by significant changes in wind direction caused by the Sistan's 120-Day Winds period, and is home to approximately 6 million people making it the second most populous province in Iran (Statistical Centre of Iran, 2011; http://www.amar.org.ir). In addition, ~19.5% of the land area of Iran affected by wind erosion is located in this province (Range and Watershed Department of Khorasan Razavi; http://www.nr-khr.ir). Loess deposits in the southern City of Mashhad (Karimi et al., 2009) and on the eastern slopes of the Kopeh Dagh mountains (Karimi et al., 2014; Okhravi and Amini, 2001) as well as extensive areas of active and stabilized sand dunes are evidence of intense past and present wind activities in this province.

Given the intensity and seasonal direction of the winds coupled with the extreme relief in this region, we hypothesize that dust deposition in Khorasan Razavi is controlled by the interaction between these winds and the location of topographic features (e.g., mountain ranges or playas). In addition, we hypothesize that the nature of these interactions changes on a monthly or seasonal timescale corresponding to atmospheric features over the region.

Our objective was to test these hypotheses by investigating the spatial and temporal distribution of modern dust in Khorasan Razavi Province as well as its relationship to atmospheric properties and distance to probable sources (e.g., playas). Because this study represents the first published measurements of dust in this region of Iran, a secondary goal was to provide baseline dust data by which to evaluate future regional anthropogenic climate and land use effects on aeolian and land surface processes.

2. Materials and methods

2.1. Study area, geographical setting, and regional atmospheric processes

Khorasan Razavi Province is located between 56.2° and 61.5° E and 33.5° to 37.7° N in north-eastern Iran (Fig. 1). Elevations range from 235 m in Sarakhs plain near the border between Iran and Turkmenistan to 3211 m at Binaloud Mountain north of the City of Neyshabur (Fig. 1). Mean annual precipitation ranges from 116 mm in Khaf to 313 mm in Quchan and mean annual temperature ranges between 12.2 °C in Fariman and 18.2 °C in Sabzevar.

The Binaloud and Kopeh Dagh mountain ranges run parallel to each other and are separated by the Mashhad plain in the northern portion of Khorasan Razavi (Fig. 1). To the east, Sarakhs loess plain is located at the base of the Kopeh Dagh Mountains. The Chehel Tan is an east-west trending bow-like mountain range situated in the center of the study area and extends from the city of Torbat-e Heydariyh to Bardskan. Several extensive playas with clay flats, salt crusts and sand dunes are present immediately south of the Chehel Tan. Neogene gypsiferous and calcareous marls are distributed in the study area (Fig. 1).

Approximately 75% of the province is located within arid or semi-arid climates (Peel et al., 2007). Meteorological stations distributed throughout the province (Fig. 1) record multiple dust storms each year, with some stations reporting occasional frequencies of 50 or more storms occurring in a single year (Islamic Republic of Iran Meteorological Organization (IRIMO), 2013).

Khorasan Razavi is under the influence of three main air masses that cause major changes in weather conditions during the year. Southern migration of the Siberian high-pressure system causes polar continental air to interact with warm moist air originating from the Atlantic Ocean and Mediterranean Sea causing precipitation during the late fall to early spring. Warm dry air masses originating north of the Caspian Sea increase temperature and decrease humidity in the region and cause Sistan's 120-Days Winds period, which increases dust production and transport from late spring to mid-summer.

According to meteorological reports and satellite observations, most stormy days in Khorasan Razavi occur in the spring. Synoptic analysis of dust storms in the province show that in the warm period of the year (late spring and summer), a low-pressure center moves over the southern areas of Khorasan Razavi and Afghanistan while the Azores High expands toward the Black and Caspian Seas increasing the meridional pressure gradient and causing heavy winds and dust storms in the region (Lashkari and Keikhosravi, 2008).

2.2. Atmospheric data

Data on wind direction, wind speed, rainfall, humidity, and temperature during the sampling period (1 May 2014–30 April 2015) were obtained at 3-hour intervals from the Iranian Meteorological Organization from 11 weather stations distributed across Khorasan Razavi (Fig. 1). At nine of the stations (Gonabad, Kashmar, Khaf, Mashhad, Neyshabur, Sarakhs, Sabzevar, Torbat-e Jam, and Torbat-e Heidariyeh) dust storm events were recorded as either dust haze, raised dust, or dust storm. These stations were located near (< 10 km) the dust trap sites. Observations of dust storms were obtained from 1985 to 2015 to investigate long-term trends in dust flux within the province.

Atmospheric visibility as affected by dust was assessed using the World Meteorological Organization (WMO) coding system that is used to record and report the amount of dust in the atmosphere (Goudie and Middleton, 2006). To examine the spatial distribution of dust storms in Khorasan Razavi, seasonal and annual changes in the number of dust storms were analyzed using the Dust Storm Index (DSI). This index provides a measure of the frequency and intensity of wind erosion events following O'Loingsigh et al. (2014). It is calculated as:

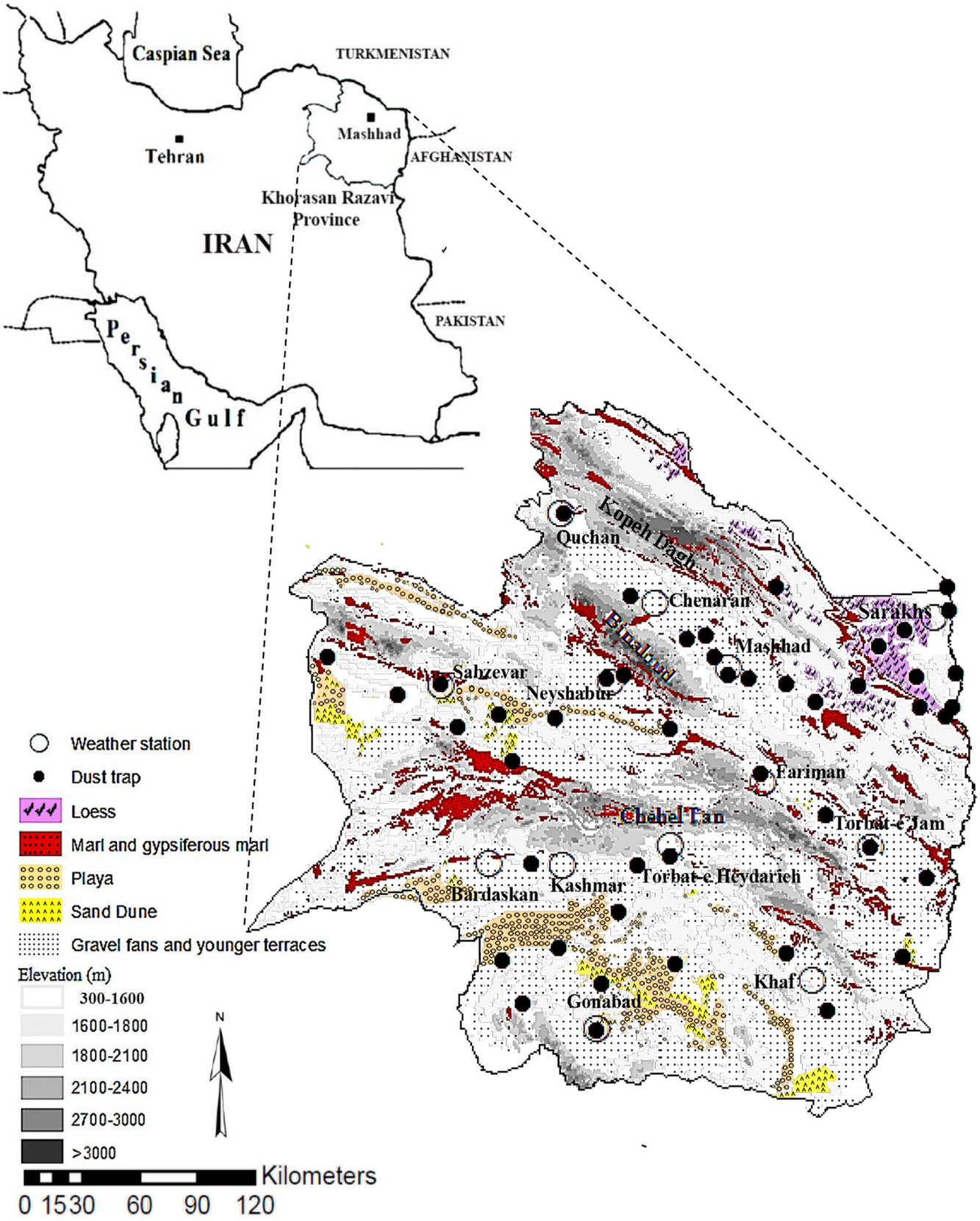

Fig. 1. Location of the study area (Khorasan Razavi Province) in northeastern Iran. Inset map shows the general location of the province. Lower map shows the distribution of dust traps, locations of weather stations and other relevant geomorphic features. Topographic and geologic information taken from the Range and Watershed Department of Khorasan Razavi (2015).

$$DSI = \sum_{i=1}^{n} [(5 \times SDS) + MDS + (0.05 \times LDE)]_i \quad (1)$$

where DSI is dust storm index at the *i*th station, *n* is the total number of stations recording a dust event observation in the time period, SDS represents severe dust storm days and is taken to be the number of days that recorded a 33, 34, or 35 on the WMO index. MDS represents moderate dust storm days and is taken to be the number of days that recorded a 30, 31, 32, or 98 as the maximum WMO index. LDE represents the number of days of local dust events with daily maximum WMO indices of 7, 8, or 9. Satellite and climate data in the province were obtained from the National Oceanic and Atmospheric Administration (NOAA) National Centers for Environmental Prediction (NCEP). We used the Hybrid Single Particle Lagrangian Integrated Trajectory (HYSPLIT) model (Stein et al., 2015) available online through NOAA (http://ready.arl.noaa.gov/HYSPLIT.php) to examine backward trajectories of air masses at each weather station during three strong dust storm events within the study period (31 May 2014, 13 June 2014, and 30 June 2014) in Khorasan Razavi.

2.3. Sampling

A total of 50 dust sampling sites were selected based on geological, geomorphological and topographical characteristics (Fig. 1). A dry flat collection tray with an area of 1 m^2, similar to that of Norouzi et al. (2017), Hojati et al. (2012), and Menendez et al. (2007) was used to sample atmospheric dust (Fig. 2). Each collection tray consisted of a glass surface (100 × 100 cm^2) covered by an overlaid 2-mm PVC mesh to form an area with a roughness suitable for trapping entrained particles (Fig. 2).

We set up the trays at an altitude of approximately three meters from the ground on flat-roofed buildings. The rooftop protected the traps from vandalism while facilitating ease of access for monthly sampling. Placement of the traps at this height also allowed the sample to remain uninfluenced by other low altitude wind processes that represent local effects. Additionally, care was taken to set the traps in areas not shaded by trees or other buildings.

Sampling sites were distributed over the province at 50 locations. Dust samples were collected monthly by using a rubber spatula to scrape off materials adhered to the glass trays. All collection trays were wet cleaned immediately following sampling. A total of 600 samples were collected from the sites between 1 May 2014 and 30 April 2015. The dry sample weight to surface area ratio of each trap (1 m^2) and the period of dust collection (30 days) were used to calculate rates of atmospheric dust flux.

2.4. Data analyses

Bivariate and time series data were plotted to assess seasonal effects on dust flux. Data were also analyzed using multiple regression on z-score transformed variables to evaluate the relative effects and identify the main factors controlling the spatial and temporal distribution of dust in the region. Dust mass and DSI data were interpolated across the province using an inverse distance weighted (IDW) algorithm in ArcGIS 9.3 (ESRI, Redlands, CA) to examine the spatial distribution of dust. IDL software version 8.5.1 was used to visualize patterns of average monthly wind speed and direction. Wind direction and speed data were visualized as wind rose plots (Fig. 3).

3. Results and discussion

3.1. Monthly atmospheric conditions

Data on monthly wind direction and speed, rainfall, humidity, and air temperature during the sampling period (May 2014 to April 2015) are presented in Table 1. The normal climate of the sampling period was based on 30-year records from 1985 to the end of 2014. We observed similar patterns in wind speed and direction over that 30-year period in the province compared with the studied period from 2014 to 2015. The mean maximum monthly temperature (36.3 °C) occurred in July 2014 and the mean minimum temperature (11.4 °C) in December 2014. Mean annual temperature for the sampling period was 16.7 °C and mean annual precipitation was 215 mm consistent with the range of these parameters for Khorasan Razavi Province. The Köppen-Geiger climate classification of the region was arid steppe cold climate (BSk) (Peel et al., 2007). A strong seasonal effect was present in the temporal distribution of precipitation with a combined mean summer rainfall (July, August, and September) across the province of < 1 mm.

Precipitation reached a maximum in March with a winter precipitation totalling 96 mm for the months of January, February, and March (Table 1). Maximum pan evaporation and lowest relative humidity were observed between June and September corresponding to the lowest mean monthly precipitation and highest temperatures. Conversely, the lowest evaporation measurements and highest relative humidity were observed during or near the winter months (i.e., December–March).

The strongest winds were observed between April and June reaching a mean maximum velocity in June of 19.5 km h^{-1}. The weakest winds were observed during September (12.4 km h^{-1}) and January (12.1 km h^{-1}) with the winter months generally showing the lowest mean maximum velocities. It is noteworthy that the strongest winds were seen in June immediately following a relatively wet period (i.e., March–May) with significantly higher precipitation and lower evaporation. The significant decline in precipitation and increase in wind speed between May (32 mm; 16.4 km h^{-1}) and June (5.4 mm; 19.5 km h^{-1}) may allow salts to concentrate on the land surface and be entrained by wind (Reheis and Urban, 2011; Reynolds et al., 2009).

Significant seasonal differences in wind direction can be observed in the 30-year wind climatologies (Fig. 4) where north-easterly winds over Turkmenistan and much of Iran dominate between the months of May and October, and westerly and north-westerly winds over the Caspian Sea and western Iran dominated from November through April (Fig. 4). Prevailing winds are also stronger from the north-easterly direction during May through October than they are during other months (Fig. 4). Direction and speed of these two winds and their relative dominance can have significant effects on the sediment accumulation in

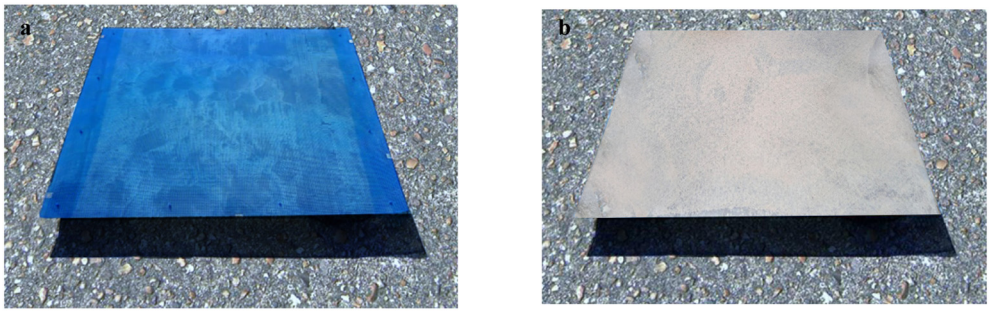

Fig. 2. Sampler used to collect airborne dust consisting of a glass surface (100 × 100 cm^2) cover and an overlaid PVC mesh with 2-mm openings following Hojati et al. (2012). These samplers were located on the roofs of buildings 5 cm above the roof surface corresponding to ~3 m above the ground level. Photographs show sampler (a) before dust deposition and (b) immediately before dust collection.

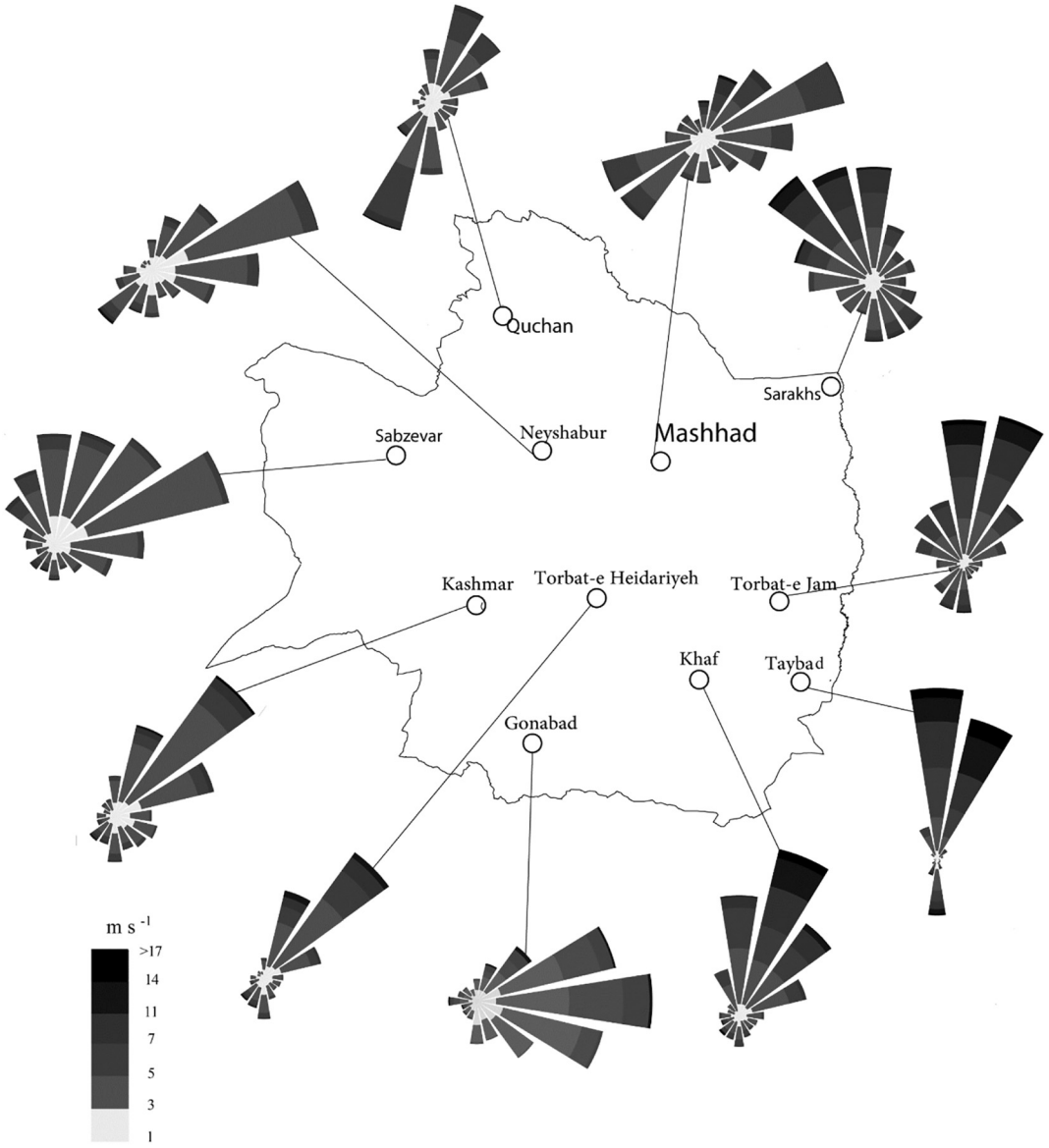

Fig. 3. Rose diagrams of wind speed and direction from 30-year normals for selected meteorological stations of Khorasan Razavi. Data were taken from meteorological stations maintained by the Iranian Meteorological Organization (https://irimo.ir). See Fig. 1 for the locations of these stations.

Table 1
Climatological parameters for the study area (Khorasan Razavi Province) averaged across all the stations shown in Fig. 1 during the period 1 May 2014 to 30 April 2015.

Year	Month	Mean monthly		Precipitation (mm)	Evaporation (mm)	Relative humidity (%)	Maximum wind speed (km h^{-1})
		Maximum (°C)	Minimum (°C)				
2014	May	28.3	14.0	32.0	260.4	36.1	16.4
2014	June	33.6	18.6	5.4	370.5	21.7	19.5
2014	July	36.3	21.3	0.6	466.5	16.8	14.3
2014	August	35.4	18.8	0.5	441.3	17.6	14.3
2014	September	32.9	15.8	0.0	343.6	20.2	12.4
2014	October	26.5	11.6	9.0	226.7	38.5	15.7
2014	November	16.0	3.3	25.0	56.9	56.3	13.2
2014	December	11.4	0.4	24.4	10.4	65.7	13.0
2015	January	11.7	0.9	19.3	0.0	61.2	12.1
2015	February	13.5	2.3	25.8	0.0	65.0	15.5
2015	March	11.2	1.2	50.8	0.0	69.7	15.6
2015	April	28.3	8.4	22.5	170.4	42.9	17.3

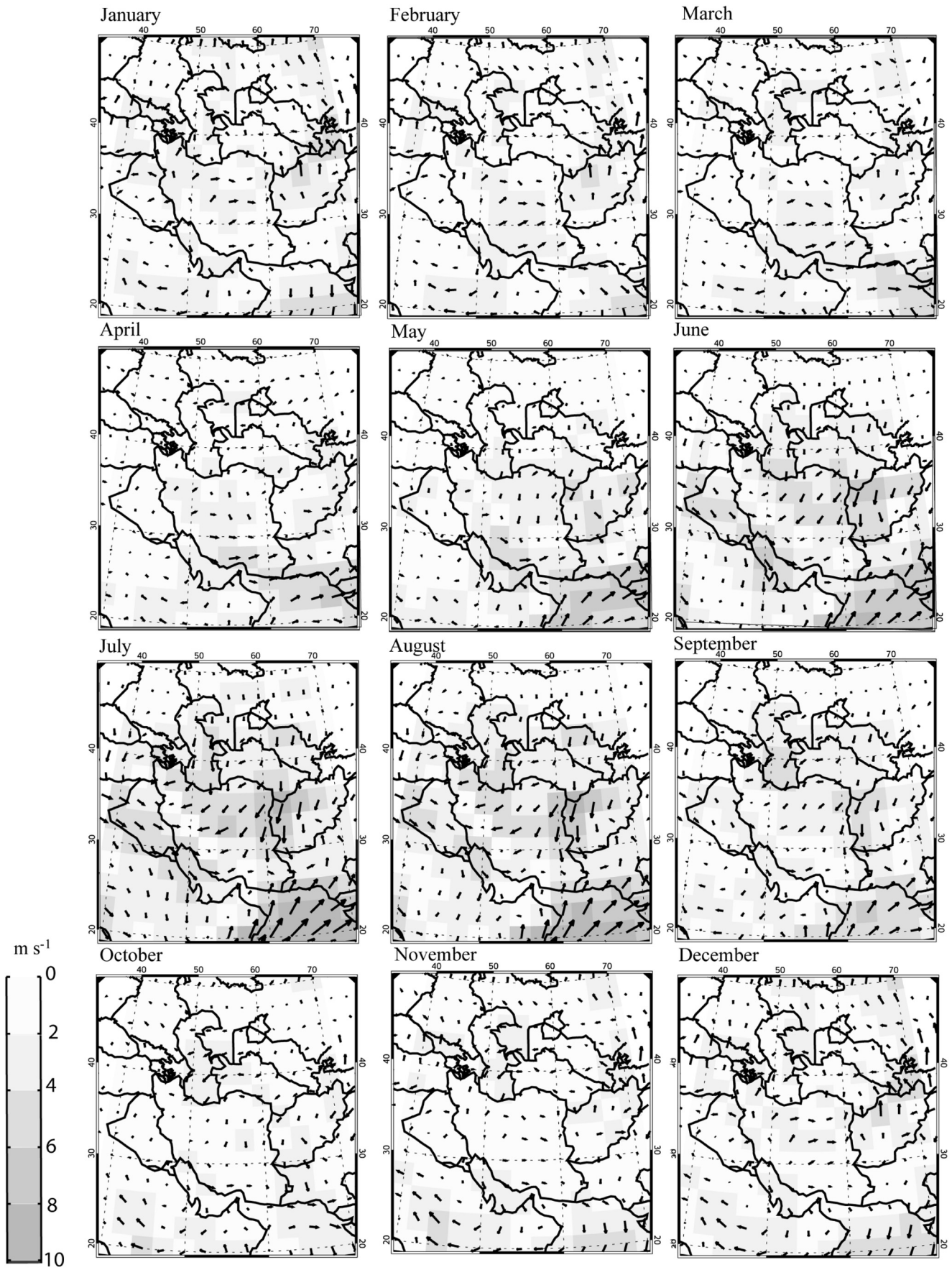

Fig. 4. Monthly near surface wind speed and direction in Iran (model sigma level of 0.995) for the 30-year normals using NCEP/NCAR reanalysis data (Kalnay et al., 1996; Kistler et al., 2001).

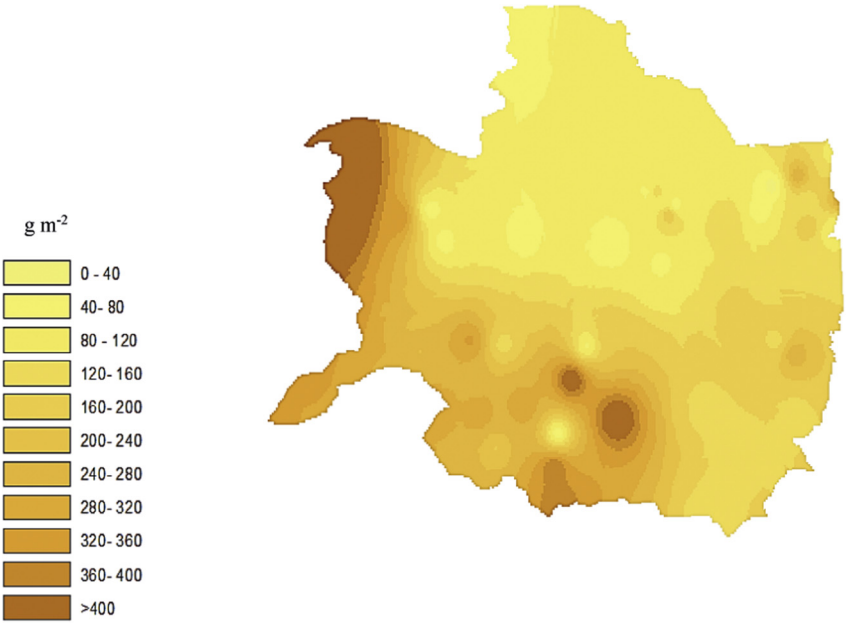

Fig. 5. Spatial distribution of annual dust fallout rate within Khorasan Razavi Province; the IDW method was used to spatially interpolate the results.

different areas of the province over different times of the year.

In the late spring and summer, winds over the plains in Turkmenistan and much of Iran are northeasterly (Rashki, 2012; Zawar-Reza et al., 2005). This wind affects the morphology of sand dunes in the eastern, western and southern portions of Khorasan Razavi (Karimi et al., 2017; Mashhadi et al., 2007) and is responsible for the loess plain, covered by aeolian dust 1–10 m thick in the northeast corner of the province (Fig. 1) (Karimi et al., 2011). The Qibla winds, which are strongest between the months of November and April, flow from southwest to northeast over Iran and collide in Khorasan Razavi with the weakened north-easterly winds during this period, causing a westerly prevailing wind direction in these months (Doostan, 2013).

3.2. Temporal and spatial distribution of dust flux

Our data showing the spatial distribution of annual atmospheric dust flux in the study area (Fig. 5) indicated that the largest dust fluxes were in the western and southwestern regions of Khorasan Razavi, likely related to the distribution of playas in the province (Fig. 1). In the north, the dust fluxes were lower due to the increased elevation of the mountainous topography in this part of the province which yields greater rainfall, increasing both atmospheric humidity and soil moisture (Hojati et al., 2012; Menendez et al., 2007).

Annual dust deposition varied considerably from $< 40\ g\ m^{-2}\ y^{-1}$ in the mountainous north to $> 400\ g\ m^{-2}\ y^{-1}$ in the western portion of the province near a vast playa found there (Fig. 5). These findings are in agreement with the results of Cao et al. (2011), who reported that fallout rates in Xi'an, Shaanxi Province, Central China, ranged from 0.005 to $450\ g\ m^{-2}\ y^{-1}$ for mountainous and desert areas, respectively. Ta et al. (2004) reported an average dust fallout rate of about $309\ g\ m^{-2}\ y^{-1}$ from a 15-year study in China and O'hara et al. (2006) found a fallout rate of $276\ g\ m^{-2}\ y^{-1}$ from a study in Libya. In a study conducted in Kuwait Bay from August 2009 to July 2010 and from August 2010 to July 2011, Neelamani and Al-Dousari (2016) estimated annual dust fallout rates of about 225 and $283\ g\ m^{-2}\ y^{-1}$, respectively. Considerably higher dust deposition rates, however, have been reported from Kuwait City at approximately $600\ g\ m^{-2}\ y^{-1}$ (Al-Awadhi and Al-Shuaibi, 2013).

Monthly atmospheric dust fluxes are shown in Fig. 6. Average dust fallout in the province varied from $9.97\ g\ m^{-2}$ in December to $20.96\ g\ m^{-2}$ in June. Maximum dust fallout with high variability ranged from $50.27\ g\ m^{-2}$ in April to $150.4\ g\ m^{-2}$ in June. The narrow range of minimum dust fluxes was $0.3\ g\ m^{-2}$ in July to $1.65\ g\ m^{-2}$ in February.

The highest dust fallout rates were observed in the western and southern parts of Khorasan Razavi Province from March to September, with the highest dust deposition occurring during the late winter and spring (Fig. 6). The largest area within the province with the highest dust fallout rate was observed in June. From July to February, the average amount of dust fallout declined while the highest rates of fallout shifted to the eastern part of the Province after September. The increase in rainfall during the last month of the autumn and during the winter in combination with the absence of internal sources of dust likely explain the low dust fallout rates during this time period.

The dust fallout rate decreased in autumn and winter across the region, except for the Sarakhs area where an increase in dust fallout rate was observed from November to February (Figs. 1 and 6). Given the high wind velocities ($> 20\ m\ s^{-1}$) during spring and summer, Sarakhs may act as a channel for winds preventing high dust deposition and cause dust to be carried over longer distances. However, during autumn and winter, wind speeds decrease causing larger dust fallout rates compared to spring and summer and according to the meteorological data, the highest dust storm in the province during fall and winter seasons occur in Sarakhs.

Overall, dust deposition in the area was relatively high. Norouzi and Khademi (2015) showed that in Isfahan (i.e., located in the center of Iran), the highest dust fallout rates occurred in July averaging $8.05\ g\ m^{-2}$ and the lowest occurred in December with an average of $2.13\ g\ m^{-2}$ compared to the monthly average value found in Khorasan Razavi of $20.96\ g\ m^{-2}$ and $9.97\ g\ m^{-2}$ in June and December, respectively. Jaafari and Khademi (2015) reported that the highest and lowest rates of airborne dust fallout in Kerman occurred on May and November corresponding to values of 17.4 and $5\ g\ m^{-2}$, respectively, with the values steadily decreasing between those months. In a study examining

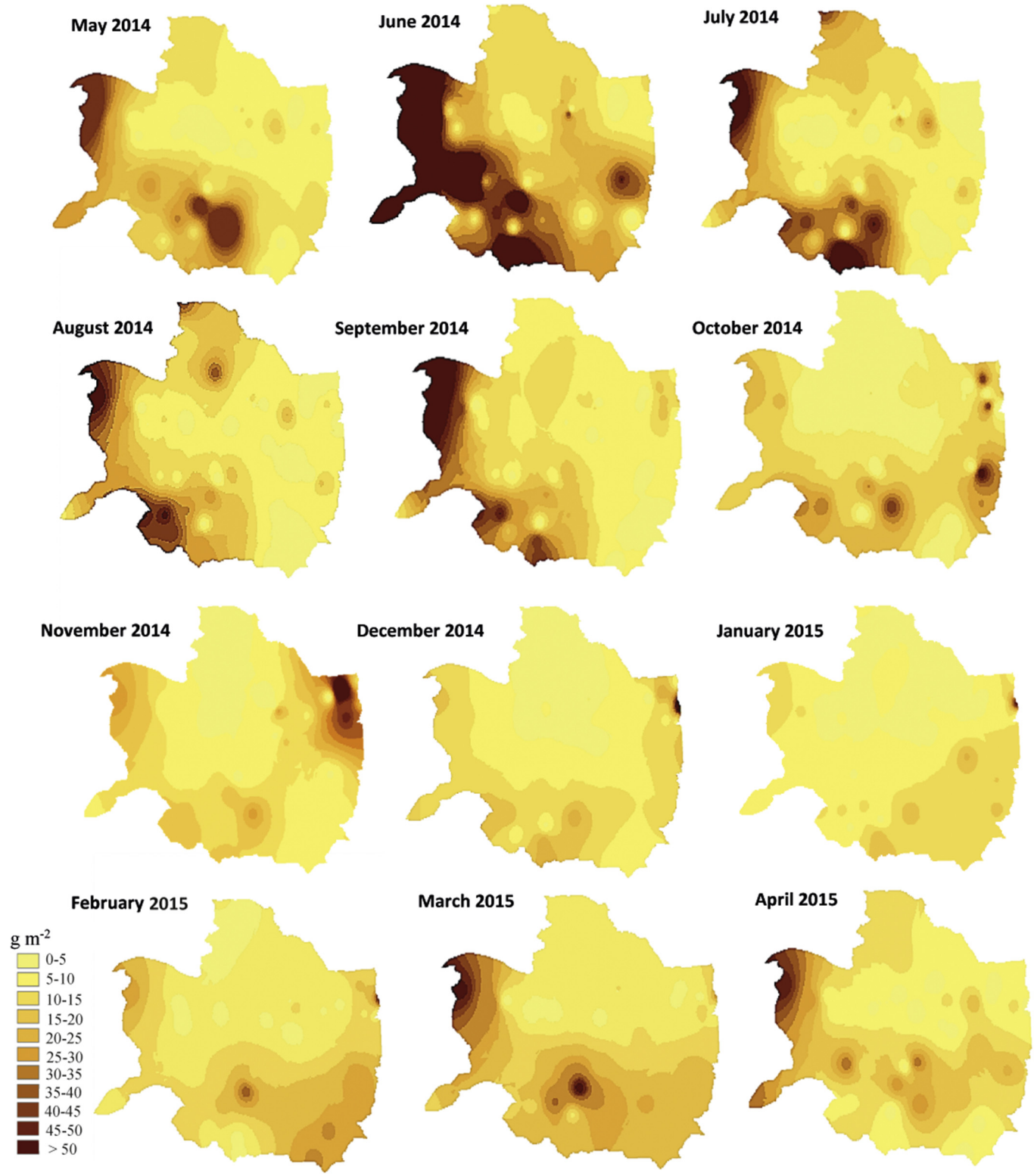

Fig. 6. Spatial distribution of monthly atmospheric dust fallout over Khorasan Razavi Province between May 2014 and April 2015.

the spatial and temporal variations of dust fallout in the city of Kermanshah, in Kermanshah Province, western Iran, Ahmadi-Doabi et al. (2013) reported average fallout rates of 19.2 and 3.3 $g\,m^{-2}$ for spring and summer, respectively.

Similarly, Al-Harbi (2015) observed the highest fallout rates in the city of Shuyoukh, Kuwait, during the months of June and August with values of 76.4 and 97.26 ± 2.5 $g\,m^{-2}\,mo^{-1}$, respectively. The lowest rates were observed in October and November at 14 ± 1.2 and 19 ± 1.4 $g\,m^{-2}\,mo^{-1}$, respectively. In addition, December, January and February had moderate dust fallout rates which ranged from 25.5 ± 1.3 to 30.5 ± 1.5 $g\,m^{-2}\,mo^{-1}$. The seasonality of these observations of dust fallout rate in Khorasan Razavi are similar to findings in the broader region.

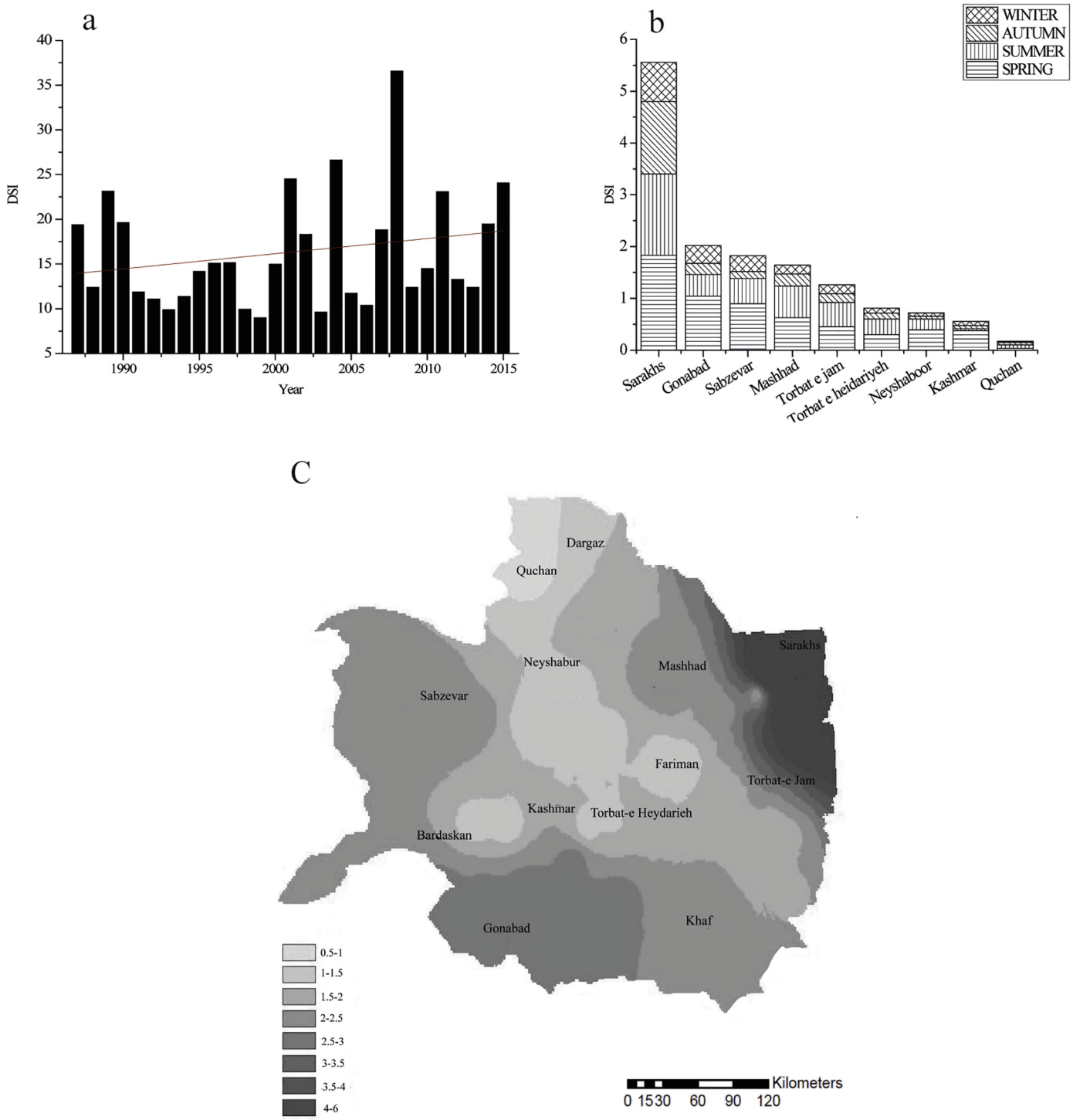

Fig. 7. (a) Variation in the annual total dust storm index (DSI) for Khorasan Razavi Province (Red line is linear regression), (b) seasonal variation of DSI, and (c) spatial variation of the DSI in Khorasan Razavi Province. Data taken from meteorological stations maintained by the Iranian Meteorological Organization (https://irimo.ir) for the period 1985–2015. Calculation of DSI follows O'Loingsigh et al. (2014).

3.3. Atmospheric controls on the distribution of dust

Fig. 7a shows an increasing trend of average total DSI computed from meteorological stations of Khorasan Razavi from 30-year normals. The highest rate of dust storms was recorded in 2008 which was related to a drought that occurred in Khorasan Razavi that year. In fact, findings from Erfanian et al. (2015) and Taherian (2015) indicate that the area is becoming more drought-prone and that drought severity is increasing over time. According to Kaskaoutis et al. (2016), the exposure of northeastern Iran to the 120-day winds creates favorable conditions for airborne dust emission. Studies of Lashkari and Keikhosravi (2008) and Doostan (2015) have also shown an increase in dust phenomena in these areas.

Using the Standardized Precipitation Index to identify drought between 2004 and 2010, Boroghani et al. (2016) showed that drought greatly increased the occurrence of dust storms in Khorasan Razavi. We recorded the highest numbers of dusty days in most regions of the province during the spring months (Fig. 7b). Spring and autumn have

the highest and lowest number of dust storms occurrences, respectively. These results are consistent with the findings of Boroghani et al. (2016), Hamidi et al. (2013) and Rezazadeh et al. (2013), who concluded that most of the dusty days in Khorasan Razavi Province occurred in spring. The city of Sarakhs recorded the highest number of dust storms in all seasons, followed by Gonabad and Sabzevar cities (Fig. 7b). According to the meteorological reports of Sarakhs station in the eastern part of Khorasan Razavi, the average wind speed was 3 m s^{-1}. At this station, the annual average number of days winds exceeded 15 m s^{-1} was 50, mostly occurring between mid-June and July. Moreover, maximum wind speeds of 22 m s^{-1} have been logged at this station. Sarakhs is situated in the lowest region of the province, in the vicinity of Turkmenistan deserts, and is characterized with flat topography and low altitudes. This low relief in combination with low mean annual precipitation accounts for the high number of dusty days experienced by Sarakhs compared to other cities in the province.

Khorasan Razavi Province receives its highest rainfall during late fall and winter decreasing toward late spring. A combination of poor vegetation coverage in the region and an increase in atmospheric temperature predisposes the spring season to dusty days. The highest and lowest dust storm and DSI occurred in Sarakhs and Quchan, respectively. The DSI increased from the center toward the margins of the province except for the northeast (Fig. 7c) probably due to the presence of mountainous topography, increased elevation, and the proximity to vast playas coupled with low atmospheric humidity. Our results are consistent with the findings of Prospero et al. (2002), who suggested that dry flat regions are more likely to experience dust storms than mountains areas.

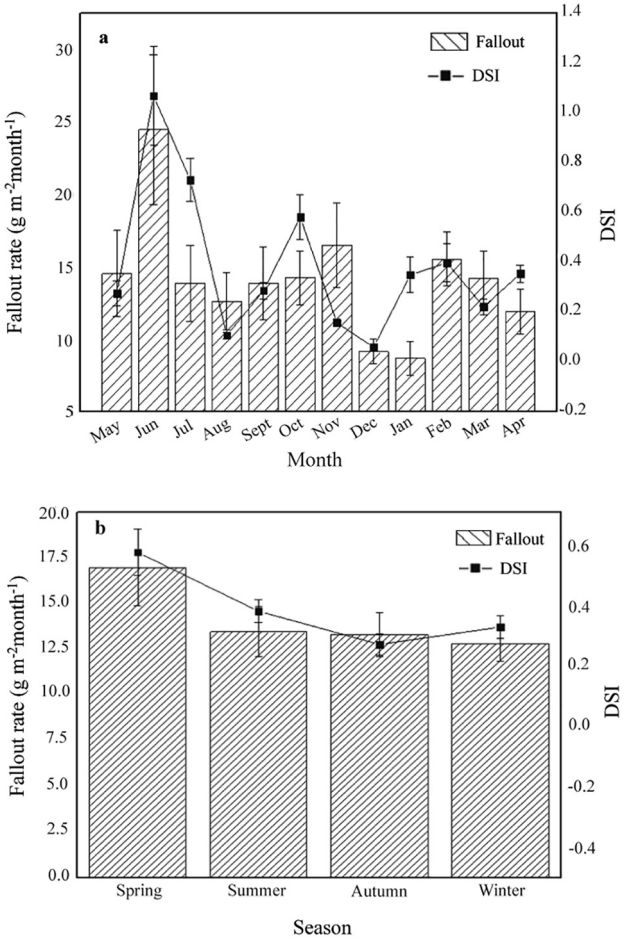

Fig. 8. (a) Average monthly and (b) seasonal dust fallout rate and DSI values in Khorasan Razavi Province (n = 144).

Monthly variability in dust fallout rates tracked the number of dust storm events (Fig. 8). Months with minimal dust storms were associated with the lowest dust deposition rates. By contrast, the maximum abundance of dust fallout was observed when soils had minimum vegetation cover and highly intense winds blowing in the region (Fig. 6).

Higher standard deviation of dust fallout rates in May and June (5.17 and 2.95 g m^{-2}) can be attributed to more frequent occurrences of dust storms during this period (Fig. 8a). Similar positive correlations between dust storm frequency and standard deviations were observed by Beitlefteh et al. (2015), Hojati et al. (2012), Liu et al. (2004), Reheis and Kihl (1995), Reheis and Urban (2011), and Ta et al. (2004).

The highest fallout rates were observed during the spring season at 16.96 ± 2.1 g m^{-2} mo^{-1} (Fig. 8b). On average, 30% of the total annual deposition accumulated during the spring. Dust deposition was approximately 23% of the total dust deposition for each summer, autumn, and winter owing to fewer dust events. Fig. 9 shows estimates of backward trajectories of air masses before several severe dust storms during spring: (1) 31th May 2014, (2) 13th June 2014, and (3) 30th June 2014. Three major routes are observable from the HYPSPLIT model for the transport of dust particles to the center of the province. Based on recent studies (Mohammadi-Moradian and Hosseinzadeh, 2016; Rashki, 2017), the northeast to southwest route is the main corridor for dust storms traveling from the Turkmenistan's desert region as well as Central-Asia down to Khorasan Razavi. Most of these events are observed in the spring and summer. The second route is from the northwest to southeast and the third route is from the southwest to northeast. The frequency of these routes corresponds to prevailing winds during the warm period of the year. Winds formed by thermal low-pressure systems, blowing from the eastern side of the region during spring have a key role in the creation and transport of local and trans-regional dust (Mohammadi-Moradian and Hosseinzadeh, 2016).

Wind speed and direction were important factors affecting the spatial and temporal distribution of fallout rates in the study area. According to Fig. 4, prevailing winds blow from the east and northeast during April to October and change directions to blow from the west and northwest during November to March. On a regional scale, the 120-day winds are one of the most important climate characteristics during warm seasons in eastern Iran. The major pressure centers, which cause the 120-day winds, are located in the north of the Caspian Sea and south of Iran. The west-east shifts of these two centers in the summer cause the expansion and intensification of these winds (Doostan, 2013). In the cold half of the year, westerly and northwesterly winds and their concomitant pressure center influence the climate of the broader region (Alijani and Houshyar, 2008). As shown in the Fig. 4 the beginning of the cold period of the year (November to March) was accompanied with the spread of westerly winds to lower latitudes which influenced ground-level atmospheric conditions (Shamsipour and Safarrad, 2011). Although the prevailing westerly winds have high speed, they do not appear to carry airborne dust from internal sources since they occur during autumn and winter when soil conditions are relatively moist.

3.4. Atmospheric-landscape-dust interactions

The correlation analysis indicated relatively low association between annual dust fallout rate and relative humidity (−0.57), precipitation (−0.37), wind speed (0.20), and temperature (0.51). Previous studies have investigated the correlation between climatic parameters and the occurrence of dust storms and reported both positive and negative correlations that vary for different geographical regions (e.g., Reheis and Kihl, 1995; Wang et al., 2004; Yu et al., 1992). These findings suggest that monthly or seasonal dust flux is not controlled by a single factor only but by several factors, which may act separately or in combination with each other. To assess the relative contribution of these factors to the temporal and spatial distribution of dust deposition in Khorasan Razavi Province, selected independent variables including meteorological parameters and distance from the

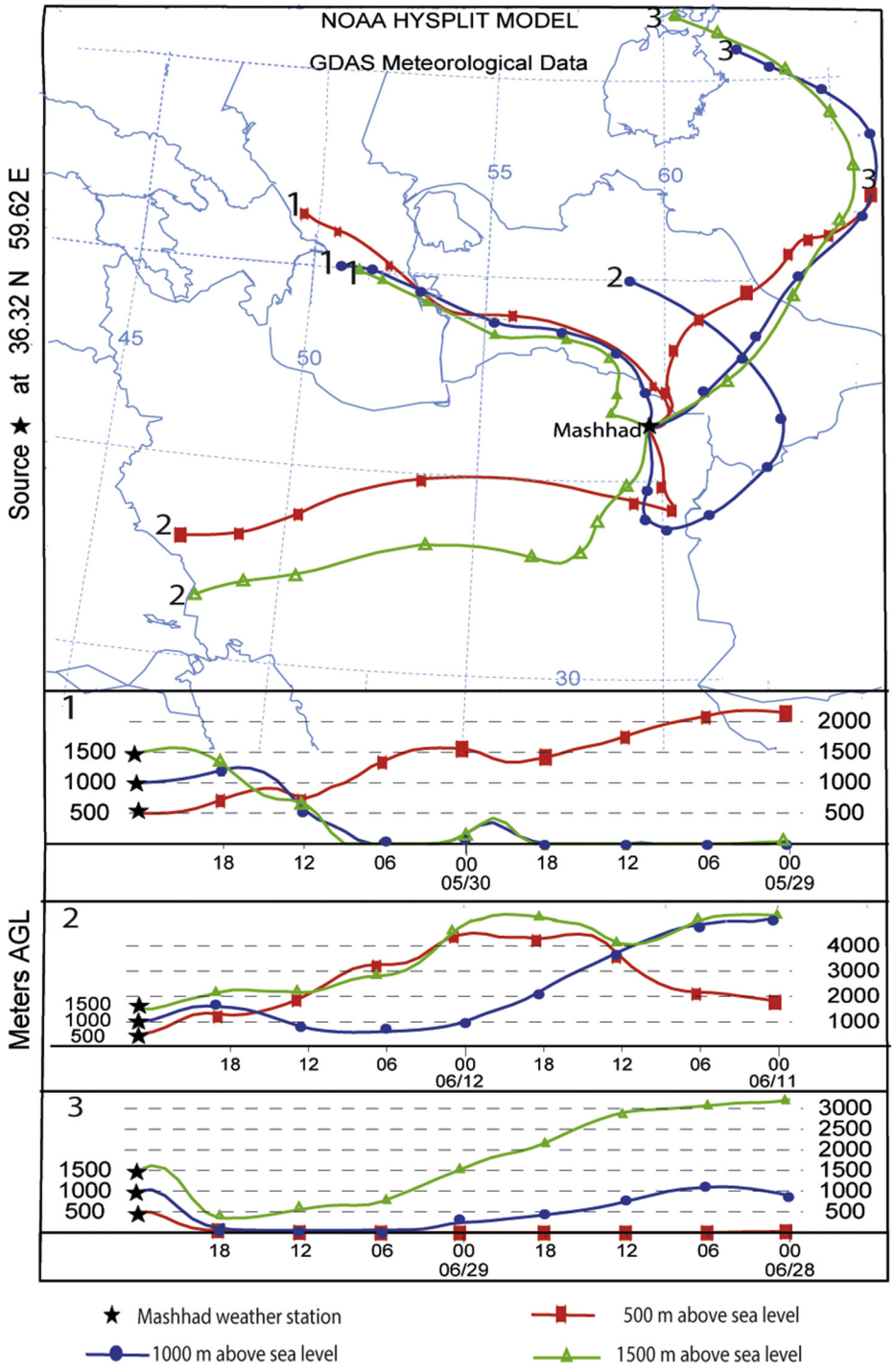

Fig. 9. Backward trajectories (48 h) of air masses before several severe dust storms during spring 2014: (1) 31 May 2014, (2) 13 June 2014, and (3) 30 June 2014. Triangle, square, and circle represent 6 h distances between points. Data were obtained from the NOAA (http://ready.arl.noaa.gov/HYSPLIT.php) and accessed 15 November 2016.

nearest playas were examined with standardized multiple linear stepwise regression. Wind velocity, temperature, humidity and distance from the nearest playa displayed the lowest covariance and explained the largest amount of variation in dust flux and were, therefore, used as input variables in the statistical model. The results obtained from this analysis are shown in Table 2.

Our results showed that distance from the nearest playa was a key factor that explained more of the variation in dust flux than climatic parameters during the months of March, May, June, and also July to September (i.e., the summer season) (Table 2). Dust was easily entrained and transported during these months because of the low relative humidity of the atmosphere in these areas and high wind speeds. By contrast, in the months with low wind speed and higher rainfall, particles could not be easily moved by wind (Okin et al., 2001; Pokharel and Kaplan, 2017). Climatological factors such as precipitation and temperature are the main controls governing dust flux in these months.

The squares of the beta weights for the winter season shown in Table 2 indicate that distance from the nearest playa explained 1.2 and 1.1 times the variation in dust deposition rate compared to average wind speed and temperature, respectively. As expected, distance from

Table 2
Results of the standardized stepwise multiple regression analysis aggregated by month and season.

Time	Equation	R^2	*P*-value
Month			
May 2014	$F_{May} = -0.002D + 1.20$	0.141	0.0084
Jun 2014	$F_{Jun} = -0.399D - 0.370$	0.316	0.0002
July 2014	$F_{Jul} = -0.059D + 21.5$	0.064	0.0828
August 2014	$F_{Aug} = -0.001D + 1.12$	0.064	0.0818
September 2014	$F_{Sep} = -0.314D + 0.279T$	0.184	0.0102
October 2014	$F_{Oct} = -0.019H + 1.73$	0.155	0.0057
November 2014	$F_{Nov} = 0.423T + 0.229W$	0.192	0.0076
December 2014	$F_{Dec} = 0.309T - 0.239P$	0.169	0.0154
January 2015	$F_{Jan} = -348H + 0.321W$	0.195	0.0075
February 2015	$F_{Feb} = 0.316T + 0.306W - 0.263D$	0.262	0.0037
March 2015	$F_{Mar} = -0.459D$	0.246	0.0017
April 2015	$F_{Apr} = -0.352P + 0.272W$	0.148	0.0270
Season			
Spring 2014	$F_{Spring} = -0.412H - 0.245D$	0.263	0.0011
Summer 2014	$F_{Summer} = -0.140D + 69.72$	0.090	0.0372
Autumn 2014	$F_{Autumn} = -1.881P + 74.84$	0.274	0.0001
Winter 2015	$F_{Winter} = -0.379D + 0.340T + 0.320W$	0.313	0.0008

Dust fallout rate (F) was logarithmically transformed prior to standardization of the variable. Climatological and landscape parameters include distance to nearest playa (D), precipitation (P), temperature (T), wind speed (W), and humidity (H). Values preceding these parameters represent beta weights.

the nearest playa was negatively correlated with dust flux while wind and temperature were positively correlated.

Playas are one of the most important sources of dust due to the high susceptibility of the land surface to wind erosion in these landforms (Cahill et al., 1996; Gill, 1996; Gill et al., 2002). The time interval between wetting and drying of playa has a direct impact on dust emissions (Fécan et al., 1998; Mckenna-Neuman and Nickling, 1989; Reynolds et al., 2007, 2009). These systems are commonly characterized by large surfaces with sparse vegetation and soft sediments that provide ideal conditions for wind and dust entrainment (Bryant, 2013; Rashki et al., 2013, 2015).

Dust fallout rate seems related to relatively humid periods, which can be identified by a lag phase of heavy precipitation. Heavy precipitation can accompany rapid dust emission. Both runoff by fresh sediment moved onto the surface of the playa and the formation of loose sediment and puffy salt crystals on the surfaces of wet playas are mechanisms that can increase dust emissions. The relatively high rainfall in wet seasons or surface moisture cause frequent changes in shallow groundwater levels which increase the potential for the formation of loose and puffy salt crystals during numerous and intermittent dissolution and sedimentation cycles on the surface of salty zones (Liu et al., 2011; Pelletier, 2008; Reheis, 2006; Reynolds et al., 2007, 2009). A similar process was observed in a Mojave Desert playa in southern California (Hirmas and Graham, 2011).

Seasonal precipitation during the sampling period causes swelling in playa sediments, which are highly susceptible to aeolian erosion after drying. In addition, rainfall causes increased heterogeneity and roughness on the surface in these areas, which increases susceptibility to aeolian erosion and the entrainment of particles due to increased friction between the wind and sediment (Webb and Strong, 2011). In dry seasons, there is a significant decrease in rainfall and the extent of formation of these loose and puffy crystals is reduced due to the presence of hard, thick and uniform salt surfaces. This causes a significant decrease in sediment dispersion and diminishes regional effects (Liu et al., 2011; Reynolds et al., 2007, 2009). Change in the atmospheric humidity, shallow ground level, and salinity of groundwater all play a significant role in playa systems. Numerous studies describe the existence of salt crusts, especially continuous, smooth-surface crusts, which often produce cemented and hard surfaces that can retard evaporation and decrease dust emission (Liu et al., 2011; Reheis, 2006; Reynolds et al., 2007, 2009).

Threshold velocity for wind erosion depends on atmospheric humidity because of its effect on the moisture content of the soil surface, which influences inter-particle cohesion (Ravi et al., 2004). Csavina et al. (2014) reported that shear-stress velocities are controlled by water sorption when the relative humidity is low.

Increases in temperature can cause decreases in soil moisture, which can decrease the speed of the threshold velocity at which surface particles are entrained by wind (Behbahani, 2006; Hussein et al., 2006; Reynolds et al., 2009). Rainfall and temperature can also play an indirect but effective role in controlling the amount of dust fallout through their effect on vegetation (Makhdoum, 2006), with changes in rainfall causing a larger effect than changes in temperature. Our results also showed that there was an association between dust generation frequency and relatively wet periods described by either heavy precipitation events or several month-long regional increased precipitation periods. Dust fluxes reached their peak in months following heavy rainfall. This is likely due to sediment carried by runoff ultimately reaching playa basins being deflated when the playa surfaces becomes desiccated (Pokharel and Kaplan, 2017; Reheis and Kihl, 1995; Reynolds et al., 2009).

4. Conclusions

Our results showed that the rate of atmospheric airborne dust fallout during the 12-month sampling period in Khorasan Razavi Province was the highest in June and lowest in December. Dust deposition rates in this province were the result of complex interactions between monthly moisture, temperature, wind velocity, and distance to a dust source.

This study showed that the rate of airborne dust fallout in the southern and western regions of the province, which border several vast playas and the Kavir Desert of central Iran, was highest during the spring season. The change in direction of prevailing winds from the east and northeast during the dry months to the west and northwest during wet months decreased the rate of airborne dust fallout in most regions, except in the east of the province where the highest wind speeds were observed in the spring and summer seasons.

In general, water content, type and thickness of crust, wind velocity, and shear stresses are the main determinants of wind erosion in the study region. Dust emission potentials of playa surfaces in this study were dynamic and changed with respect to these variables. In our study, distance to playa sources was the most important factor explaining the temporal and spatial distribution of dust flux.

The importance of hydrological effects on dust emissions from playas was also observed. Antecedent precipitation, either locally or regionally, results in the creation of wet conditions, which, in turn, likely lead to the dissolution of a salt cement and creation of puffy and loose sediments. Also, local flooding of playas create new sources of dust, such as fresh sediment, which increase surface vulnerability to wind erosion making playa surfaces susceptible to deflation during strong wind events. Future work should more carefully examine the dynamic properties of playa surfaces along with the monitoring of atmospheric conditions in Khorasan Razavi Province to more accurately predict and understand the transport and deposition of dust in this important region of Iran.

References

Ahmadi-Doabi, S., Afyuni, H., Karami, M., Khademi, H., 2013. Dust fallout rate in Kermanshah Province during spring and summer of 2013. In: The 3rd Conference on Wind Erosion and Dust Storms. Jan 2014. Yazd University, Yazd, Iran, (In Persian).
Al-Awadhi, J.M., Al-Shuaibi, A.A., 2013. Dust fallout in Kuwait City: deposition and characterization. Sci. Total Environ. 461/462, 139–148.
Al-Harbi, M., 2015. Characteristics and composition of the falling dust in urban environment. Int. J. Environ. Sci. Technol. 12, 641–652.
Alijani, B., Houshyar, M., 2008. Identification of synoptic patterns of drastic cold in north-

western Iran. J. Res. Nat. Geog. 6, 1–16 (In Persian).
Behbahani, A., 2006. Investigation and Determination of Movement of the Fluent Sands on the Desert Roads and their Control (Case Study: Yazd - Meibod Road). M.Sc. Thesis. Faculty of Natural Resources. University of Tehran (In Persian).
Beitlefteh, R., Landi, A., Hojati, S., Sayyad, G.h., 2015. Deposition rate, mineralogy and size distribution pattern of dust particles collected around the Houralazim Marshland, Khuzestan Province. J. Water Soil 29, 695–707 (In Persian).
Boroghani, M., Moradi, H.R., Zangane Asadi, M.A., 2016. Analysis of the dust occurrence and zoning in Khorasan Razavi Province. J. Environ. Eros. Res. 4, 45–57 (In Persian).
Bryant, R., 2013. Recent advances in our understanding of dust source emission processes. Prog. Phys. Geogr. 37, 397–421.
Cahill, T.A., Gill, T.E., Reid, J.S., Gearhart, E.A., Gillette, D.A., 1996. Saltating particles, playa crusts and dust aerosols at Owens (dry) Lake, California. Earth Surf. Process. Landf. 21, 621–639.
Cao, Z., Yang, Y., Lu, J., Zhang, J., 2011. Atmospheric particle characterization, distribution, and deposition in Xi'an, Shaanxi Province, Central China. Environ. Pollut. 159, 577–584.
Chow, J.C., Watson, J.G., Houck, J.E., Pritchett, L.C., Rogers, C.F., Frazier, C.A., Egami, R.T., Ball, B.M., 1994. A laboratory resuspension chamber to measure fugitive dust size distributions and chemical compositions. Atmos. Environ. 28, 3463–3481.
Csavina, J., Field, J., Félix, O., Corral-Avitia, A.Y., Sáez, A.E., Betterton, E.A., 2014. Effect of wind speed and relative humidity on atmospheric dust concentrations in semi-arid climates. Sci. Total Environ. 487, 82–90.
Department of Khorasan Razavi, 2015. http://www.nr-khr.ir.
Doostan, R., 2013. Identifying effective pressure centers on 120-day wind of Sistan and Baluchestan. In: The First National Conference of Climatology, Kerman, Iran, (In Persian).
Doostan, R., 2015. Analysis of the droughts Iran in the past half century. In: National Conference on Meteorology, Yazd, Iran, (In Persian).
Engelbrecht, J.P., Jayanty, R.K.M., 2013. Assessing sources of airborne mineral dust and other aerosols, in Iraq. Aeolian Res. 9, 153–160.
Engelstaedter, S., Tegen, I., Washington, R., 2006. North African dust emissions and transport. Earth-Sci. Rev. 79, 73–100.
Erfanian, M., Ansari, H., Alizadeh, A., Banayan-Aval, M., 2015. Assessment of climatic extreme events variations in Khorasan Razavi Province. Iran. J. Irrig. Drain. 8, 817–825 (In Persian).
Fécan, F., Marticorena, B., Bergametti, G., 1998. Parameterization of the increase of the aeolian erosion threshold wind friction velocity due to soil moisture for arid and semi-arid areas. Ann. Geophys. 17, 149–157.
Flagg, C.B., Neff, J.C., Reynolds, R.L., Belnap, J., 2014. Spatial and temporal patterns of dust emissions (2004–2012) in semi-arid landscapes, southeastern Utah, USA. Aeolian Res. 15, 31–43.
Gill, T.E., 1996. Eolian sediment generated by anthropogenic disturbance of playas: human impacts on the geomorphic system and geomorphic impacts on the human system. Geomorphology 17, 207–228.
Gill, T.E., Gillette, D.A., Niemeyer, T.C., Winn, R.T., 2002. Elemental geochemistry of wind-erodible playa sediments, Owens Lake, California. Nucl. Instrum. Methods Phys. Res., Sect. B 189, 209–213.
Goudie, A.S., Middleton, N.J., 2006. Desert Dust in the Global System, First Ed. Springer Verlag, Berlin.
Griffin, D.W., Kellogg, C.A., Shinn, E.A., 2001. Dust in the wind: long range transport of dust in the atmosphere and its implications for global public and ecosystem health. Glob. Chang. Hum. Health 2, 20–33.
Grobéty, B., Gieré, R., Dietze, V., Stille, P., 2010. Airborne particles in the urban environment. Elements 6, 229–234.
Groll, M., Opp, C., Aslanov, I., 2013. Spatial and temporal distribution of the dust deposition in Central Asia—results from a long-term monitoring program. Aeolian Res. 9, 49–62.
Hamidi, M., Kavianpour, M.R., Shao, Y., 2013. Synoptic analysis of dust storms in the Middle East. Asia-Pac. J. Atmos. Sci. 49, 279–286.
Hirmas, D.R., Graham, R.C., 2011. Pedogenesis and soil-geomorphic relationships in an arid mountain range, Mojave Desert, CA. Soil Sci. Soc. Am. J. 75, 192–206.
Hirmas, D.R., Graham, R.C., Kendrick, K.J., 2011. Soil-geomorphic significance of land surface characteristics in an arid mountain range, Mojave Desert, USA. Catena 87, 408–420.
Hojati, S., Khademi, H., Faz Cano, A., Landi, A., 2012. Characteristics of dust deposited along a transect between central Iran and the Zagros Mountains. Catena 88, 27–36.
Hussein, T., Karppinen, A., Kukkonen, J., Harkonen, J., Aalto, P.P., Hameri, K., Kerminen, V.M., Kumala, M., 2006. Meteorological dependence of size-fractionated number concentrations of urban aerosol particles. Atmos. Environ. 40, 1427–1440.
Islamic Republic of Iran Meteorological Organization (IRIMO), 2013. http://www.irimo.ir.
Jaafari, F., Khademi, H., 2015. Evaluating the rate of atmospheric dust deposition in different locations of Kerman City. J. Water Soil Sci. 18, 207–217 (In Persian).
Kalnay, E., Kanamitsu, M., Kistler, R., Collins, W., Deaven, D., Gandin, L., Iredell, M., Saha, S., White, G., Woollen, J., Zhu, Y., Chelliah, M., Ebisuzaki, W., Higgins, W., Janowiak, J., Mo, K.C., Ropelewski, C., Wang, J., Leetmaa, A., Reynolds, R., Jenne, R., Joseph, D., 1996. The NCEP/NCAR 40-year reanalysis project. Bull. Am. Meteorol. Soc. 77, 437–471.
Karimi, A., Khademi, H., Kehl, M., Jalalian, A., 2009. Distribution, lithology and provenance of peridesert loess deposits in northeast Iran. Geoderma 148, 241–250.
Karimi, A., Frechen, M., Khademi, H., Kehl, M., Jalalian, A., 2011. Chronostratigraphy of loess deposits in northeast Iran. Quat. Int. 234, 124–132.
Karimi, A., Soodmand, A., Khormali, F., 2014. Grain size parameters of aeolian deposits in Sarakhas area, Norteastern Iran. In: International Symposium on Loess, Soils and Climate Change in Southern Eurasia. Gorgan.
Karimi, A., Khormali, F., Wang, X., 2017. Discrimination of sand dunes and loess deposits using grain-size analysis in northeastern Iran. Arab. J. Geosci. 10, 275.
Kaskaoutis, D.G., Houssos, E.E., Rashki, A., Francois, P., Legrand, M., Goto, D., Bartzokas, A., Kambezidis, H.D., Takemura, T., 2016. The Caspian Sea–Hindu Kush Index (CasHKI): a regulatory factor for dust activity over southwest Asia. Glob. Planet. Chang. 137, 10–23.
Kistler, R., Kalnay, E., Collins, W., Saha, S., White, G., Woollen, J., Chelliah, M., Ebisuzaki, W., Kanamitsu, M., Kousky, V., Dool, H.V.D., Jenne, R., Fiorino, M., 2001. The NCEP–NCAR 50–year reanalysis: monthly means CD–ROM and documentation. Bull. Am. Meteorol. Soc. 82, 247–267.
Lashkari, H., Keikhosravi, Q., 2008. Synoptic analysis of dust storms in Razavi Khorasan Province in the period 1993–2005. J. Nat. Geog. Res. 65, 17–33 (In Persian).
Liu, L.Y., Shi, P.J., Gao, S.Y., Zou, X.Y., Erdon, H., Yan, P., Li, X.Y., Ta, W.Q., Wang, J.H., Zhang, C.L., 2004. Dustfall in China's western loess plateau as influenced by dust storm and haze events. Atmos. Environ. 38, 1699–1703.
Liu, W., Abuduwaili, J., Lei, J.Q., Wu, G.Y., 2011. Deposition rate and chemical composition of the aeolian dust from a bare saline playa, Ebinur Lake, Xinjiang, China. Water Air Soil Pollut. 218, 175–184.
Mahmoudi, Z., 2011. Geochemical and Mineralogical Characterization of Atmospheric Dust. M.S. Thesis of Soil Science. Faculty of Agriculture, Isfahan University of Technology (In Persian).
Makhdoum, M., 2006. Fundamental of Land-use Planning, Sixth Ed. (Tehran, Iran. (In Persian)).
Marx, S.A., McGowan, H.A., 2005. Dust transportation and deposition in a super humid environment, West Coast, South Island, New Zealand. Catena 59, 147–171.
Mashhadi, N., Ahmadi, H., Ekhtesasic, M.R., Feizniab, S., Feghhid, G., 2007. Analysis of sand dunes to determine wind direction and detect sand source sites (case study: Khartooran Erg, Iran). Desert 12, 69–75.
Mckenna-Neuman, C., Nickling, W.G., 1989. A theoretical and wind tunnel invistigatioh of effect of capillary water on the entrainment of sediment by wind. Can. J. Soil Sci. 69, 79–96.
McTainsh, G.H., 1999. Dust transport and deposition. In: Goudie, A., Livingstone, S., Stokes, I. (Eds.), Aeolian Environments, Sediments and Landforms. John Wiley and Sons, Ltd, Chichester, pp. 181–211.
Menendez, I., Diaz-Hernandez, J.L., Mangas, J., Alonso, I., Sanchez-Soto, P.J., 2007. Airborne dust accumulation and soil development in the North-East sector of Gran Canaria (Canary Islands, Spain). J. Arid Environ. 71, 57–81.
Mohammadi-Moradian, J., Hosseinzadeh, S.R., 2016. Synoptic analysis and satellite monitoring of dust storms in Mashhad: a case study during 2003–2013. Q. Geog. Environ. Hazards. 4, 35–57 (In Persian).
Neelamani, S., Al-Dousari, A., 2016. A study on the annual fallout of the dust and the associated elements into the Kuwait Bay, Kuwait. Arab. J. Geosci. 9, 210.
Norouzi, S., Khademi, H., 2015. Spatial and temporal variations of rate of airborne dust fallout in Isfahan city and its relationship with climatic factors. J. Sci. Technol. Agric. Nat. Res. 72 Water and Soil Science. (161-149 (In Persian)).
Norouzi, S., Khademi, H., Ayoubi, S., Faz Cano, A., Acosta, J.A., 2017. Seasonal and spatial variations in dust deposition rate and concentrations of dust-borne heavy metals, a case study from Isfahan, central Iran. Atmos. Pollut. Res. 8, 686–699.
O'hara, S.L., Clarke, M.L., Elatrash, M.S., 2006. Field measurements of desert dust deposition in Libya. Atmos. Environ. 40, 3881–3897.
Okhravi, R., Amini, A., 2001. Characteristics and provenance of the loess deposits of the Gharatikan watershed in Northeast Iran. Glob. Planet. Chang. 28, 11–22.
Okin, G.S., Murray, B., Schlesinger, W.H., 2001. Degradation of sandy arid shrub land environments: observations, process modeling, and management implications. J. Arid Environ. 47, 123–144.
O'Loingsigh, T., McTanish, G.H., Tews, E.K., Strong, C.L., Leys, J.F., Shinkfield, P., Tapper, N.J., 2014. The Dust Storm Index (DSI): a method for monitoring broad scale wind erosion using meteorological records. Aeolian Res. 12, 29–40.
Peel, M.C., Finlayson, B.L., Mcmahon, T.A., 2007. Updated world map of the Köppen-Geiger climate classification. Hydrol. Earth Syst. Sci. 4, 439–473.
Pelletier, J.D., 2008. Quantitative Modeling of Earth Surface Processes, First Ed. Cambridge University.
Pokharel, A.K., Kaplan, M.L., 2017. Dust climatology of the NASA Dryden Flight Research Center (DFRC) in Lancaster, California, USA. J. Clim. 5, 15–33.
Prospero, J.M., Ginoux, P., Torres, O., Nicholson, S.E., Gill, T.E., 2002. Environmental characterization of global sources of atmospheric soil dust identified with the Nimbus 7 total ozone mapping spectrometer (TOMS) absorbing aerosol product. Rev. Geophys. 40, 2–31.
Rashki, A., 2012. Seasonality and Mineral, Chemical and Optical Properties of Dust Storms in the Sistan Region of Iran, and Their Influence on Human Health. Ph.D. Thesis. Faculty of Natural and Agricultural Sciences, University of Pretoria.
Rashki, A., 2017. Atmospheric Dynamics, Properties and Transportation of Dust Storms Over the Southwest Asia (From the Caspian Sea to the Arabian Sea) LoessFest 2017, October. University of Gorgan, Gorgan, Iran.
Rashki, A., Kaskaoutis, D.G., Rautenbach, C.J.deW., Eriksson, P.G., Qiang, M., Gupta, P., 2012. Dust storms and their horizontal dust loading in the Sistan region, Iran. Aeolian Res. 5, 51–62.
Rashki, A., Erikson, P.G., Rautenbach, C.J.deW., Kaskaoutis, D.G., Grote, W., Dykstra, J., 2013. Assessment of chemical and mineralogical characteristics of airborne dust in the Sistan region, Iran. Chemosphere 90, 227–236.
Rashki, A., Kaskaoutis, D.G., Francois, P., Kosmopoulos, P.G., Legrand, M., 2015. Dust-storm dynamics over Sistan region, Iran: seasonality, transport characteristics and affected areas. Aeolian Res. 16, 35–48.
Ravi, S., D'Odorico, P., Over, T.M., Zobeck, T.M., 2004. On the effect of air humidity on soil susceptibility to wind erosion: the case of air-dry soils. Geophys. Res. Lett. 31 (L09501).

Reheis, M.C., 2006. A 16-year record of aeolian dust in Southern Nevada and California, USA: controls on dust generation and accumulation. J. Arid Environ. 67, 487–520.
Reheis, M.C., Kihl, R., 1995. Dust deposition in southern Nevada and California, 1984–1989: relations to climate, source area, and source lithology. J. Geophys. Res. 100, 8893–8918.
Reheis, M.C., Urban, F.E., 2011. Regional and climatic controls on seasonal dust deposition in the southwestern U.S. Aeolian Res. 3, 3–21.
Reynolds, R.L., Yount, J.C., Reheis, M.C., Goldstein, H., Chavez Jr, P., Fulton, R., Whitney, J., Fuller, Ch., Forester, R.M., 2007. Dust emission from wet and dry playas in the Mojave Desert, USA. Earth Surf. Process. Landf. 32, 1811–1827.
Reynolds, R.L., Bogle, R., Vogel, J., Goldstein, H., Youn, J., 2009. Dust emission at Franklin Lake Playa, Mojave Desert (USA): response to meteorological and hydrologic changes 2005–2008. Nat. Resourc. Environ. Stu. 15, 105–115.
Rezazadeh, M., Irannejad, P., Shao, Y., 2013. Climatology of the Middle East dust events. Aeolian Res. 10, 103–109.
Shamsipour, A.A., Safarrad, T., 2011. Satellite and synoptic analysis of dust storm in Western half of Iran (Case Study: July 2009). Physic. Geog. Res. 79, 111–126 (In Persian).
Shao, Y.P., 2008. Physics and Modelling of Wind Erosion, Second Ed. Springer, Heidelberg.
Statistical Center of Iran (SCI), 2011. http://www.amar.org.ir.
Stein, A.F., Draxler, R.R., Rolph, G.D., Stunder, B.J.B., Cohen, M.D., Ngan, F., 2015. NOAA's HYSPLIT atmospheric transport and dispersion modeling system. Bull. Am. Meteorol. Soc. 96, 2059–2077.
Ta, W., Xiao, H., Qu, J., Xiao, Z., Yang, G., Wang, T., Zhang, X., 2004. Measurements of dust deposition in Gansu Province, China, 1986–2000. Geomorphology 57, 41–51.
Taherian, M., 2015. Analysis of Temperature Trend Changes in Khorasan Razavi and Northern Khorasan Provinces. M.S. Thesis of Climatology. Faculty of Literature and Human Science, Islamic Azad University, Central Tehran Branch, Iran (In Persian).
Wang, X., Dong, Z., Zhang, J., Liu, L., 2004. Modern dust storms in China: an overview. J. Arid Environ. 58, 559–574.
Wang, X., Dong, Z., Zhang, C., Qian, G., Luo, W., 2009. Characterization of the composition of dust fallout and identification of dust sources in arid and semiarid North China. Geomorphology 112, 144–157.
Webb, N.P., Strong, C.L., 2011. Soil erodibility dynamics and its representation for wind erosion and dust emission models. Aeolian Res. 3, 165–179.
Wiggs, G.F.S., O'hara, S.L., Wegerdt, J., Van der Meer, J., Small, I., 2003. The dynamics and characteristics of aeolian dust in dryland Central Asia: possible impacts on human exposure and respiratory health in the Aral Sea basin. Geogr. J. 169, 142–157.
Xuan, J., Sokolik, I.N., Hao, J., Guo, F., Mao, H., Yang, G., 2004. Identification and characterization of sources of atmospheric mineral dust in East Asia. Atmos. Environ. 38, 6239–6252.
Yu, B., Nell, D.T., Hesse, P.P., 1992. Correlation between rainfall and dust occurrence at Mildura, Australia: the difference between local and source area rainfalls. Earth Surf. Process. Landf. 17, 723–727.
Yu, H., Remer, L.A., Chin, M., Bian, H., Tan, Q., Yuan, T., Zhang, Y., 2012. Aerosols from overseas rival domestic emissions over North America. Science 337, 566–569.
Zawar-Reza, P., Kingham, S., Pearce, J., 2005. Evaluation of a year-long dispersion modelling of PM_{10} using the mesoscale model TAPM for Christchurch, New Zealand. Sci. Total Environ. 349, 249–259.